DYNAMIC ANALYSIS AND NATURAL FREQUENCIES OF PLANAR AND SPATIAL SPRING-LOADED CABLE-LOOP-DRIVEN PARALLEL MECHANISMS

Hanwei Liu and Clément Gosselin
Département de génie mécanique, Université Laval, Québec, QC, Canada.
Email: hanwei.liu.1@ulaval.ca; gosselin@gmc.ulaval.ca

ABSTRACT

The dynamic analysis of novel architectures of planar and spatial spring-loaded cable-loop driven parallel mechanisms is introduced in this paper. First, the geometry of the mechanisms is briefly described and the inverse kinematic equations are given. Then, the cable forces are obtained for both the static and dynamic conditions. Due to the cable loops in the mechanisms, cables might become slack when the end-effector moves with high acceleration. Therefore, it should be verified that the cables can be maintained in tension for a certain range of trajectory frequency. Based on the static force and the Newton-Euler formulation, the natural frequencies and the corresponding ratio of the amplitudes for these two mechanisms are also found.

Keywords: cable-loop-driven parallel mechanism; dynamics; natural frequency.

ANALYSE DYNAMIQUE ET FRÉQUENCES NATURELLES DE MÉCANISMES PARALLÈLES PLANS ET SPATIAUX ENTRAÎNÉS PAR BOUCLES DE CÂBLES

RÉSUMÉ

L'analyse dynamique de nouvelles architectures de mécanismes parallèles plans et spatiaux entraînés par boucles de câbles est présentée dans cet article. Tout d'abord, la géométrie des mécanismes est brièvement décrite et les équations cinématiques sont données. Ensuite, on en déduit les forces dans les câbles pour des conditions statiques et dynamiques. En raison des boucles de câbles dans les mécanismes, les câbles pourraitent se relâcher lors du déplacement de l'effecteur avec de fortes accélérations. Par conséquent, il convient de vérifier que les câbles puissent être maintenus en tension pour une certaine plage de fréquence de trajectoire. En utilisant l'expression des efforts statiques et la formulation de Newton-Euler, la fréquence naturelle et le rapport des amplitudes correspondant à ces deux mécanismes sont également présentés.

Mots-clés : mécanismes parallèles entraînés par boucles de câbles ; dynamique ; fréquence naturelle.

1. INTRODUCTION

In conventional cable-driven parallel mechanisms, one end of each of the cables is wound on a fixed actuated drum while the other end is attached to the end-effector. Several issues arise in the design and control of cable-driven parallel mechanisms including workspace, dynamics and vibrations. In [1, 2], static models are used to obtain the wrench-closure workspace (force-closure workspace) while the so-called dynamic workspace is considered in [3]. The dynamic analysis of fully restrained cable-driven parallel mechanisms is studied in [4] while the dynamic analysis of the KNTU cable-driven parallel mechanism is studied in [5]. When large accelerations are performed, the compliance of the cables must be accounted for in order to properly predict the behaviour of the mechanism. In [6], the vibrations of general 6-DOF cable-driven parallel manipulators caused by cable flexibility are analyzed using natural frequencies. Similarly, the elastic deformation and the damping behaviour are considered in the dynamic model proposed in [7].

All the above cited works deal with conventional cable-driven parallel mechanisms. Most conventional cable-driven parallel mechanisms are redundantly actuated due to the unilaterality of the cable forces. However, alternative transmission strategies have been recently proposed in order to alleviate the drawbacks of fixed spool transmissions and actuation redundancy. In [8], the MARIONET cable-driven robot using linear actuators was presented. Also, a Cartesian cable-driven mechanism was introduced in [9], that consists of a rigid-link Cartesian skeleton frame and a cable driven system which forms a cable loop that only requires three actuators to control the three DOFs. In order to avoid actuation redundancy, sometimes gravity[10, 12], dynamic forces[11] or passive springs [12] are also applied in the mechanism.

Based on the same motivation, a modular spring-actuator cable-loop system was introduced and applied to a planar spring-loaded cable-loop-driven parallel mechanism in [13]. The main objective of this modular system is to avoid actuation redundancy by introducing compliance between the end effector and the actuator while ensuring that the mechanism remains rigid with respect to external forces until the preload of the system is exceeded. The modular spring-actuator cable-loop system is also applied to a spatial mechanism in [14]. In these mechanisms, cables form loops and a spring is attached in each cable loop. Such actuating modules depart significantly from conventional cable-driven mechanisms. Therefore, the dynamics and vibration analyses reported in the literature do not apply.

In this paper, a dynamic analysis of the cable-loop-driven parallel mechanisms introduced in [13, 14] is presented. First, the inverse kinematics and the static analysis are recalled. Then, a dynamic model is proposed. The model is then used to determine the frequency range in which the mechanism can operate. Finally, the natural frequencies and the corresponding amplitude ratios are found based on the static cable forces and the Newton-Euler formulation.

2. INVERSE KINEMATICS

Demonstration models of the planar and spatial spring-loaded cable-loop-driven parallel mechanisms are shown in Fig. 1. The mechanisms are now briefly described for the sake of completeness of this paper. More details can be found in [13] and [14].

The structure of the basic spring-loaded cable loop on which the mechanisms are based is shown in Fig. 2. Referring to Fig. 2 — which represents schematically the i^{th} loop of a cable-loop-driven mechanism — spring N_iH_i is attached to the ground at point N_i. Two pulleys C_{i1} and C_{i2} are connected to the other end of the spring at H_i. Each cable loop passes around these pulleys and the fixed pulleys to complete the loop. The loop is closed on the end-effector P. The cable loops are driven by linear actuators M_i. The cable segments A_iC_{i1}, D_iC_{i1}, $C_{i1}H_i$, J_iH_i and the spring H_iN_i are parallel to each other. The cable segments D_iE_i, $C_{i2}E_i$, J_iC_{i2} and $C_{i2}F_i$ are also parallel to each other. The positions of the fixed pulleys A_i and B_i can be expressed as $\mathbf{a}_i$ and $\mathbf{b}_i$ respectively. The lengths of the cable segments $C_{i1}H_i$, $C_{i2}J_iH_i$, $M_iD_iC_{i1}A_iP$ and $M_iE_iC_{i2}F_iG_iB_iP$ are constant. If one length of the cable segments $D_iC_{i1}A_iP$ or $E_iC_{i2}F_iG_iB_iP$ decreases, the other will increase

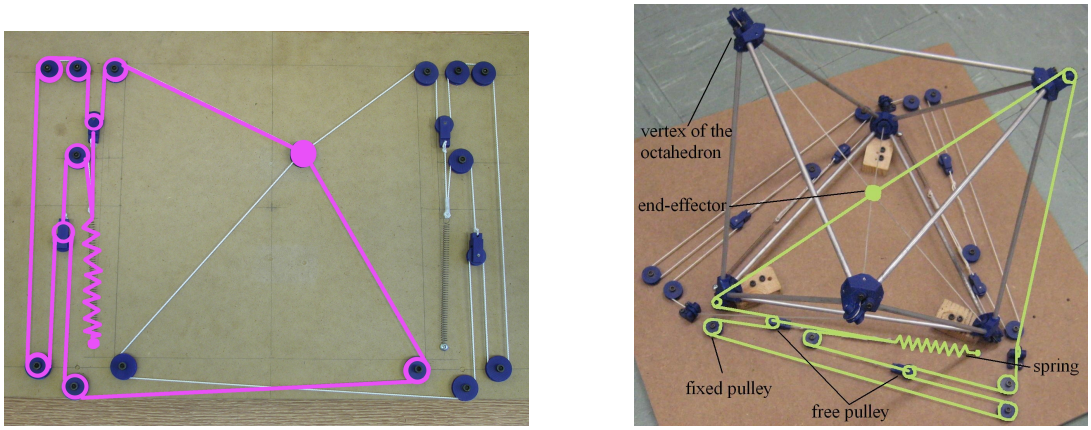

(a) Planar mechanism (b) Spatial mechanism

Figure 1. Demonstration models of the planar and spatial spring-loaded cable-loop-driven parallel mechanisms, one of the loops is highlighted.

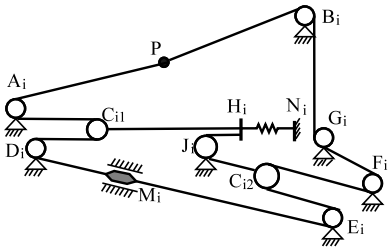

Figure 2. Schematic representation of one spring-loaded cable-loop.

by the same amount as the actuator is moving, due to the closed cable loop. The number of fixed pulleys in one loop of the spatial mechanism is different from the number of fixed pulleys included in one loop of the planar mechanism but the operating mode is the same.

The structure of the planar mechanism is shown in Fig. 3. The mechanism comprises two spring-loaded cable loops. The loops are arranged symmetrically. The four fixed pulleys A_i and B_i, $i = 1,2$, form a square. The spatial mechanism comprises three spring-loaded cable loops as shown in the demonstration model, the fixed pulleys through which the cables pass first from the end-effector form an octahedron as shown in Fig. 4.

The lengths of the cable segments PA_i and PB_i vary according to the position of point P and these variations are induced by the displacement of the actuators and the deformation of the springs. The reference position is taken as the centre of the square or of the octahedron. Assuming the reference position of the end-effector to be $\mathbf{p}_o$, for the i^{th} cable loop we have

$$2\delta_i - l_{mi} = |PA_i| - |P_oA_i|, \tag{1}$$

$$2\delta_i + l_{mi} = |PB_i| - |P_oB_i|, \tag{2}$$

where l_{mi} is the displacement of the ith actuator and δ_i is the deformation of the ith spring. With these

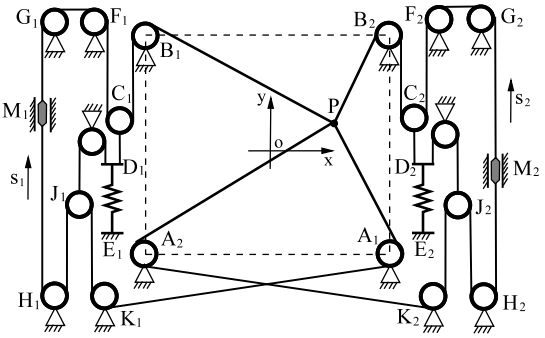

Figure 3. Schematic representation of the symmetric 2-DOF spring-loaded cable-loop-driven parallel mechanisms.

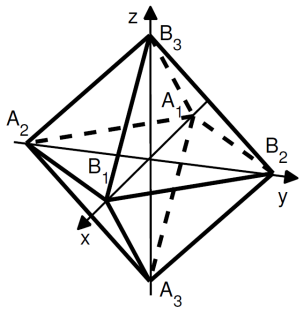

Figure 4. Octahedron formed by the six fixed pulleys.

equations (Eqs. (1) and (2)), l_{mi} and δ_i can be found as

$$\begin{aligned} \delta_i &= \frac{1}{4}(n_{ai}+n_{bi}), \\ l_{mi} &= \frac{1}{2}(n_{bi}-n_{ai}), \end{aligned}$$

where $n_{ai} = |PA_i| - |P_oA_i|$, $n_{bi} = |PB_i| - |P_oB_i|$.

Differentiating the expressions for l_{mi}, the velocity equation and the acceleration expression can be found as

$$\begin{aligned} \dot{\mathbf{l}}_m &= \mathbf{J}_l\dot{\mathbf{p}}, \\ \ddot{\mathbf{l}}_m &= \mathbf{J}_l\ddot{\mathbf{p}} + \mathbf{K}_l\dot{\mathbf{p}}, \end{aligned}$$

where

$$\mathbf{J}_l = -\frac{1}{2}(\mathbf{S}_b - \mathbf{S}_a)^T, \quad \mathbf{K}_l = -\frac{1}{2}\left[\begin{array}{cc} \frac{\partial(\mathbf{S}_b-\mathbf{S}_a)^T}{\partial x}\dot{\mathbf{p}} & \frac{\partial(\mathbf{S}_b-\mathbf{S}_a)^T}{\partial y}\dot{\mathbf{p}} \end{array} \right].$$

The unit vectors defined along the direction of the cable segments going from the end-effector to the fixed pulleys through which the cables first pass are noted $\mathbf{s}_{ai}$ and $\mathbf{s}_{bi}$, with

$$\mathbf{s}_{ai} = \frac{\mathbf{a}_i - \mathbf{p}}{||\mathbf{a}_i - \mathbf{p}||}, \qquad \mathbf{s}_{bi} = \frac{\mathbf{b}_i - \mathbf{p}}{||\mathbf{b}_i - \mathbf{p}||}$$

and matrices $\mathbf{S}_a = [\mathbf{s}_{a1}, \ldots, \mathbf{s}_{aj}]$, $\mathbf{S}_b = [\mathbf{s}_{b1}, \ldots, \mathbf{s}_{bj}]$ are formed with these vectors, where $j = 2$ for the planar mechanism and $j = 3$ for the spatial mechanism.

From the above equations, it can be observed that the inverse kinematic equations only depend on the position, velocity and acceleration of the end-effector and are independent from the external forces, assuming that the cables are all under tension.

3. STATIC ANALYSIS

Neglecting friction between the cable and pulleys, the cable forces f_{ai}, f_{bi} in the cable segments between the actuators and the end-effector are assumed to be uniform. Considering the static equilibrium of the end-effector, we have

$$\mathbf{S}_a\mathbf{f}_a + \mathbf{S}_b\mathbf{f}_b = \mathbf{f}_e \tag{3}$$

where $\mathbf{f}_a = [f_{a1}, f_{a2}, f_{a3}]^T$ and $\mathbf{f}_b = [f_{b1}, f_{b2}, f_{b3}]^T$ are the forces in the cable segments and $\mathbf{f}_e = [f_{ex}, f_{ey}, f_{ez}]^T$ is the external force applied on the end-effector. For the planar mechanism, $f_{a3} = f_{b3} = f_{ez} = 0$ and vectors $\mathbf{f}_a$, $\mathbf{f}_b$ and $\mathbf{f}_e$ have only two components.

The relationship between the ith spring force, f_{si}, and its deformation, δ_i, is assumed to be given by

$$f_{si} = f_{oi} + k_i\delta_i, \tag{4}$$

where f_{oi} is the preload and k_i is the stiffness of the spring. Also, it can be observed that the forces in the springs are independent from the external forces. If the cables are all under tension, according to the geometry of the mechanism, the spring forces and the cable forces have the following relationship:

$$\mathbf{f}_s = 2\mathbf{f}_a + 2\mathbf{f}_b, \tag{5}$$

where $\mathbf{f}_s = [f_{s1}, f_{s2}]^T$ for the planar mechanism and $\mathbf{f}_s = [f_{s1}, f_{s2}, f_{s3}]^T$ for the spatial mechanism.

For one cable loop, one has $f_{si} = 2f_{ai} + 2f_{bi}$ which is the result of the coupling between the two sides of the loop, as illustrated in Fig. 5. The sum of the cable forces f_{ai} and f_{bi} is equal to one half of the spring force f_{si} according to Eq. (5). However, the cable forces f_{ai} and f_{bi} vary for different external forces. Since the reference configuration is in the centre of the square or the octahedron, the i^{th} spring must be extended in most configurations (the configurations that are not on the corresponding diagonal). Depending on the sign of the stiffness of the springs, this extension results in a larger($k > 0$) or smaller($k < 0$) force f_{si} (see Eq. (4)). It can be observed that in order to keep the mechanism within its working range, the maximum available force in a cable loop is $f_{si}/2$ (see also Fig. 5).

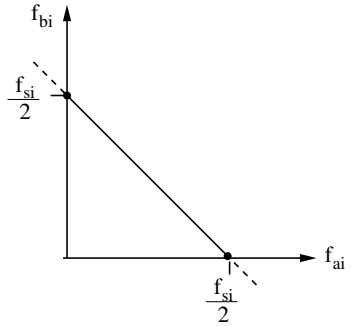

Figure 5. Illustration of $f_{si} = 2f_{ai} + 2f_{bi}$ for a given configuration.

Rewriting Eq. (5) as $\mathbf{f}_a = \frac{\mathbf{f}_s}{2} - \mathbf{f}_b$ and substituting $\mathbf{f}_a$ into Eq. (3), one has

$$\mathbf{M}_b\mathbf{f}_b = \mathbf{f}_{be} \tag{6}$$

where $\mathbf{M}_b = \mathbf{S}_b - \mathbf{S}_a$ and $\mathbf{f}_{be} = \mathbf{f}_e - \frac{1}{2}\mathbf{S}_a\mathbf{f}_s$. The equations that allow one to calculate the cable forces $\mathbf{f}_a$ are obtained using the same method. Combining the equations for $\mathbf{f}_a$ and $\mathbf{f}_b$, one has

$$\mathbf{M}\mathbf{f} = \mathbf{f}_f \tag{7}$$

where

$$\mathbf{M} = \begin{bmatrix} -\mathbf{M}_b & \mathbf{0} \\ \mathbf{0} & \mathbf{M}_b \end{bmatrix}, \quad \mathbf{f} = \begin{bmatrix} \mathbf{f}_a \\ \mathbf{f}_b \end{bmatrix}, \quad \mathbf{f}_f = \begin{bmatrix} \mathbf{f}_{ae} \\ \mathbf{f}_{be} \end{bmatrix},$$

and $\mathbf{f}_{ae} = \mathbf{f}_e - \frac{1}{2}\mathbf{S}_b\mathbf{f}_s$.

When the mechanism is in static equilibrium, the actuating force $\mathbf{f}_m$ can be written as

$$\mathbf{f}_m = \mathbf{f}_a - \mathbf{f}_b$$

where $\mathbf{f}_m = [f_{m1}, f_{m2}]^T$ for the planar mechanism and $\mathbf{f}_m = [f_{m1}, f_{m2}, f_{m3}]^T$ for the spatial mechanism.

4. DYNAMIC MODEL

The dynamic equations of the mechanism provide the relationships between actuation and end-effector forces acting on the mechanism and the acceleration and motion trajectories that result. Usually, cable-driven parallel mechanisms have simpler dynamic models than link-driven parallel mechanisms because the mass of the cables can be neglected. Dynamic equations of motion can be obtained from the Lagrangian formulation or the Newton-Euler formulation. Here, the Newton-Euler formulation is used to obtain the dynamic equations of the planar and spatial spring-loaded cable-loop-driven parallel mechanisms.

It is first assumed that the masses of the springs and the free pulleys are small enough to be neglected. Neglecting the friction between the cables and pulleys and considering only the mass of the end-effector m_p and the mass of the actuators m_m, the forces acting at the end-effector and on the moving fixtures and pulleys f_{ai}, f_{bi} are assumed to be uniform. The dynamic equations for the end-effector and the actuators can be found as

$$\mathbf{M}_m\ddot{\mathbf{l}}_m = \mathbf{f}_b - \mathbf{f}_a + \mathbf{f}_m, \tag{8}$$

$$\mathbf{M}_p\ddot{\mathbf{p}} = \mathbf{S}_a\mathbf{f}_a + \mathbf{S}_b\mathbf{f}_b. \tag{9}$$

where $\mathbf{M}_m$ and $\mathbf{M}_p$ are the mass matrix of the actuator and the end-effector, respectively. Assuming that the actuators have the same mass m_m and that the mass of the end-effector is m_p, then $\mathbf{M}_m = m_m\mathbf{E}$ and $\mathbf{M}_p = m_p\mathbf{E}$ where $\mathbf{E}$ is the identity matrix, which is of dimension 2×2 for the planar mechanism, 3×3 for the spatial mechanism.

From Eqs. (9) and (5), the cable forces $\mathbf{f}_a$, $\mathbf{f}_b$ can be found as

$$\begin{bmatrix} \mathbf{f}_a \\ \mathbf{f}_b \end{bmatrix} = \begin{bmatrix} \mathbf{E} + \mathbf{S}_{ba}^{-1}\mathbf{S}_a & -\mathbf{S}_{ba}^{-1} \\ -\mathbf{S}_{ba}^{-1}\mathbf{S}_a & \mathbf{S}_{ba}^{-1} \end{bmatrix} \begin{bmatrix} \frac{1}{2}\mathbf{f}_s \\ \mathbf{M}_p\ddot{\mathbf{p}} \end{bmatrix} \tag{10}$$

since matrix $\mathbf{S}_{ba} = \mathbf{S}_b - \mathbf{S}_a$ is always invertible within the square or the octahedron which is formed by the fixed pulleys A_i and B_i. When the cable forces $\mathbf{f}_a$ and $\mathbf{f}_b$ are known, the actuating force $\mathbf{f}_m$ can be found using the dynamic equation of the actuators, Eq. (8), as

$$\mathbf{f}_m = \frac{1}{2}(\mathbf{S}_b - \mathbf{S}_a)^{-1}(\mathbf{S}_a + \mathbf{S}_b)\mathbf{f}_s - 2(\mathbf{S}_b - \mathbf{S}_a)^{-1}\mathbf{M}_p\ddot{\mathbf{p}} + \mathbf{M}_m(\mathbf{J}_l\ddot{\mathbf{p}} + \mathbf{K}_l\dot{\mathbf{p}}). \tag{11}$$

Moreover, the modular actuator-spring systems are all assumed to have the same characteristics, i.e., $f_o = f_{oi}$ and $k = k_i$. Then, the cable extension forces f_{ai} and f_{bi} have the same properties for each mechanism.

Since cables can only operate in tension, not compression, it should be verified that the cable forces $\mathbf{f}_a$ and $\mathbf{f}_b$ remain positive for certain families of trajectories of the end-effector. Then, the frequency limitation for the mechanisms can be found. In order to preserve symmetry, the origin of the fixed coordinate frame $O-xy$ is located at the centre of the rectangle $A_1A_2B_1B_2$ for the planar mechanism and the fixed coordinate frame for the spatial mechanism is also located at the centre of the octahedron as shown in Fig. 4. The expressions appearing in Eq. (10) are rather complicated. In order to get some basic dynamic characterics of the mechanisms, it is assumed that the quadrilateral of the planar mechanism is a square with $2r$ side length and the regular octahedron of the spatial mechanism has a diagonal length $2a$.

5. FEASIBLE FREQUENCY RANGE AND REQUIRED ACTUATING FORCE

The static workspace of the planar mechanism always includes the line segments connecting the corresponding centre points of the four sides of the square. Varifying the spring characteristics, the direction of maximum change of the workspace is along the diagonals of the square [13]. For the spatial mechanism [14], the static workspace is like a ball with six bumps which point to the six pulleys on the diagonal directions. From the numerical results, it can be observed that the largest variation of the workspace boundary caused by the variation of the springs stiffness is the along the diagonal directions of the octahedron. The inscribed sphere of the octahedron (the radius is $\frac{\sqrt{3}}{3}a$) is always included in the workspace. It is intended to find the frequency range of operation and the required actuating force for the sinusoidal trajectories in special directions.

Substituting the expression of the prescribed trajectory into the cable force equations in dynamic conditions, Eq. (10), and ensuring that the cable forces are positive, inequalities relating the trajectory parameters and the spring characteristics can be obtained. The maximum trajectory frequency can be found based on all the inequalities and considering the physical meanings of the parameters. Then, substituting the trajectory with the feasible maximum frequency into the actuating force equations, Eq. (11), the required maximum actuating force can be obtained as the largest extremum value of these equations.

The analysis reveals that the maximum feasible frequency for the centre line directions of the planar mechanism is

$$\omega_{max} = \sqrt{\frac{f_o}{m_p r}} \frac{\sqrt{2+\frac{kr}{2f_o}(1+\sqrt{5}-2\sqrt{2})}}{\sqrt[4]{5}},$$

while the maximum required actuating force can be written as

$$f_{m,max} = \left[\frac{4}{5} + (\frac{1}{5} + \frac{\sqrt{5}}{5} - \frac{2\sqrt{2}}{5})\frac{kr}{f_o}\right] \frac{m_m f_o}{m_p}.$$

The maximum feasible frequency of the sinusoidal trajectory with an amplitude r in the diagonal direction and the required maximum actuating force are

$$\omega_{max} = \sqrt{\frac{f_o}{m_p r}\left[(\frac{1}{2} + \frac{1}{2\sqrt{3}}) + \frac{kr}{4f_o}(1-\sqrt{\frac{2}{3}})\right]},$$

$$f_{m,max} = f_o(1-\frac{\sqrt{3}}{3}) + \frac{m_m f_o}{m_p}\left[(\frac{1}{2} + \frac{1}{2\sqrt{3}}) + \frac{kr}{f_o}(\frac{1}{4} - \frac{\sqrt{2}}{4\sqrt{3}})\right].$$

For the centre line direction of the spatial mechanism, the maximum trajectory frequency and actuating

force for the moving range of the inscribed sphere diameter is

$$\omega_{max} = \sqrt{\frac{f_o}{m_p a}\left[\frac{3\sqrt{2}}{2} + \frac{ka}{4f_o}(3+\sqrt{3}-3\sqrt{2})\right]},$$

$$f_{m,max} = \frac{f_o}{2}(1+\frac{m_m}{m_p})\left[1+\frac{ka}{4f_o}(\sqrt{2}+\frac{\sqrt{6}}{3}-2)\right].$$

For the diagonal direction, the trajectory of the end-effector is prescribed as

$$\mathbf{p} = \lambda a \sin(\omega t)\mathbf{e},$$

where $\lambda > 0$ and $\mathbf{e}$ is one of the unit vectors along the three coordinate axes. Then, the maximum trajectory frequency can be determined as

$$\omega_{max} = \sqrt{\frac{f_o}{m_p a}}\sqrt{\frac{\sqrt{1+\lambda^2}+2\lambda+\frac{ka}{f_o}\lambda(\sqrt{1+\lambda^2}-1)}{2\lambda\sqrt{1+\lambda^2}}}, \qquad s.t. \quad \lambda \in (0,\frac{\sqrt{3}}{3}), \qquad \frac{ka}{f_o} < 0.$$

$$f_{m,max} = (\frac{1}{2}+\frac{m_m}{2m_p})f_o + \frac{m_m\lambda}{m_p\sqrt{1+\lambda^2}}f_o\left[1+\frac{\rho}{2}(\sqrt{1+\lambda^2}-1)\right].$$

The sine curve trajectories on the two special directions were used to get the basic requirements of the mechanism's parameters. However, there are many kinds of trajectories and it is not sufficient to limit ourselves to special directions. In the following section, the natural frequency is analyzed.

6. NATURAL FREQUENCY

The natural frequency and the corresponding amplitude ratios are obtained based on the Newton-Euler formulation using the static forces for certain configurations.

The dynamic equation for the end-effector Eq. (9) can be rewritten as

$$\mathbf{g} = \mathbf{S}_a\mathbf{f}_a + \mathbf{S}_b\mathbf{f}_b = \mathbf{M}_p\ddot{\mathbf{p}} \tag{12}$$

where $\mathbf{g} = [g_1(x,y), g_2(x,y)]^T$ for the planar mechanism, $\mathbf{g} = [g_1(x,y,z), g_2(x,y,z), g_3(x,y,z)]^T$ for the spatial mechanism. The cable forces under static conditions can be obtained using Eq. (7). Assuming that f_{ai} and f_{bi}, $i = 1,2$, are constant and substituting them into the Taylor series expansion of the initial end-effector dynamic equation (Eq. (12)), the above dynamic equations become partial differential equations in x and y. Rearranging these equations, we get

$$\mathbf{M}_p\ddot{\mathbf{p}} + \mathbf{G}\dot{\mathbf{p}} = \mathbf{0} \tag{13}$$

where

$$\mathbf{G} = \frac{\partial \mathbf{g}}{\partial \mathbf{p}}.$$

Assuming $\mathbf{p}_p = [x_p e^{st}, y_p e^{st}, z_p e^{st}]^T$ (the last component is omitted for the planar mechanism), and substituting into the above equation, we get

$$(s\mathbf{M}_p + \mathbf{G})\mathbf{p}_p = \mathbf{0}$$

This equation is satisfied for any $\mathbf{p}_p$ if

$$s\mathbf{M}_p + \mathbf{G} = \mathbf{0}.$$

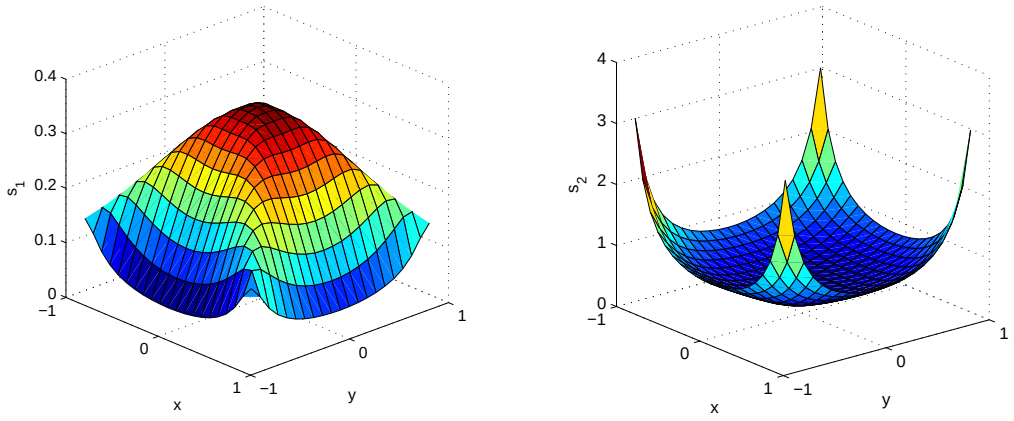

(a) Plot of s_1 (b) Plot of s_2

Figure 6. Plots of the natural frequencies of the planar mechanism with constant force springs.

In other words, the natural frequencies s_i are related to the eigenvalues of matrix $\mathbf{G}$, and the eigenvectors of matrix $\mathbf{G}$ corresponding to the value of the natural frequencies are the amplitude ratios.

It can therefore be shown that the natural frequencies at the reference position of the mechanisms are all equal. For the planar mechanism, the two natural frequencies at the reference configuration are

$$s_{io} = \frac{f_o}{2\sqrt{2}m_p r}, \qquad i = 1,2.$$

The three natural frequencies at the reference configuration for the spatial mechanism are

$$s_{io} = \frac{af_o}{m_p}, \quad i = 1,2,3.$$

Normalizing the parameters for the planar mechanism as $r = 1$, $m_p = 1$, $f_o = 1$, and assuming that the springs are constant force springs, then the two natural frequencies are shown in Fig. 6. The corresponding amplitude ratios are shown in Fig. 7. In these figures, the small black dots represent the position of the end-effector and the small line segments represent the corresponding ratio of the amplitudes. If the stiffness of the springs is not zero, the shape of surfaces corresponding to the two natural frequencies are similar to the surfaces shown in Fig. 6. Also, the natural frequencies increase when the stiffness of the springs is increased.

Normalizing the parameters of the spatial mechanism as $a = 1$ and $m_p = 1$, and assuming that the springs are constant force springs with $f_o = 10$, the natural frequencies for $z = 0$ and $z = \pm 0.2$ are shown in Fig. 8.

It can be observed, from these figures that the difference between the natural frequencies increases when the configuration is moved away from the reference position. Since the reference position of the end-effector lies in the centre of the workspace [13, 14], the mechanisms should work below the smallest natural frequency in order to avoid uncontrolled vibrations.

7. CONCLUSIONS

The dynamic analysis of cable-loop driven parallel mechanisms was addressed in this paper. Such mechanisms cannot be analyzed using the dynamic models found in the literature because of the closed-loop cable architecture. Therefore, a new model was developed based on the Newton-Euler formulation. The

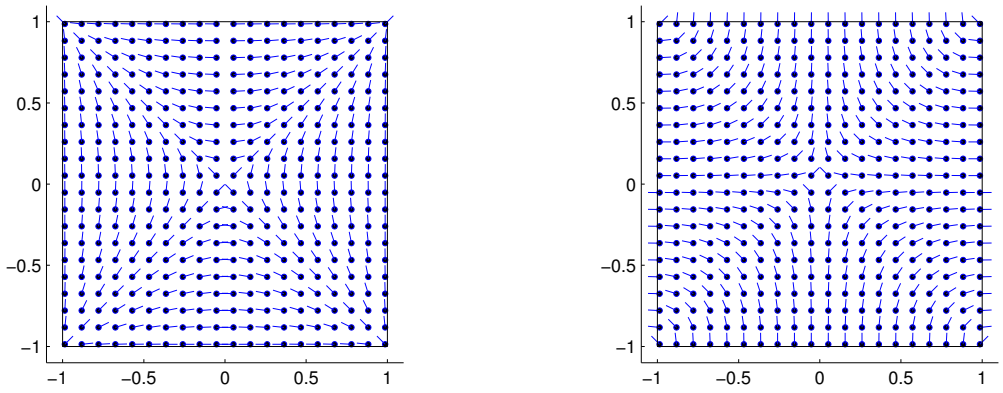

(a) ratio of the amplitudes for s_1

(b) ratio of the amplitudes for s_2

Figure 7. Ratio of the amplitudes for the planar mechanism with constant force springs.

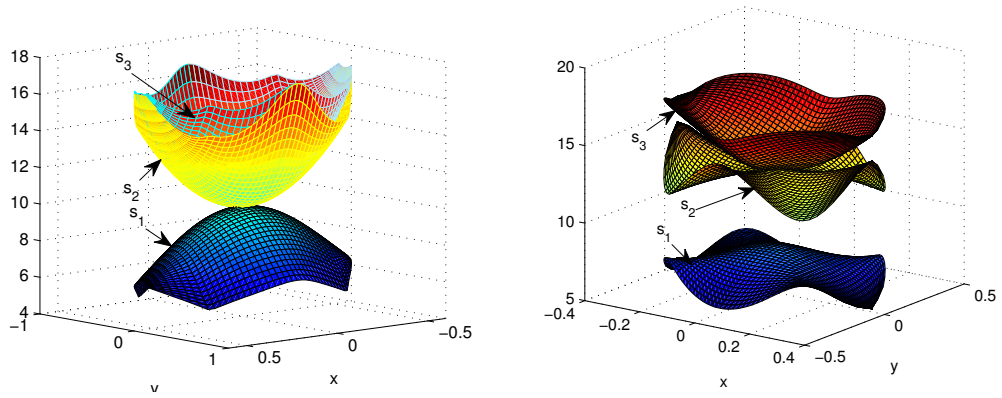

(a) $z = 0$

(b) $z = \pm 0.2$

Figure 8. The three natural frequencies of the spatial mechanism.

dynamic model obtained was used to determine the frequency limitations of fundamental trajectories in order to assess the capabilities of the mechanisms. The natural frequencies and the amplitude ratios were also found. The results obtained provide insight into the dynamic behaviour of the mechanisms and can be used as design aids. Future work includes the design of actuated prototypes.

8. ACKNOWLEDGEMENTS

The authors would like to acknowledge the financial support of the Natural Sciences and Engineering Research Council of Canada (NSERC) as well as the Canada Research Chair program.

REFERENCES

1. M. Gouttefarde, J-P. Merlet and D. Daney, 2006, "Determination of the wrench-closure workspace of 6-DOF parallel cable-driven mechanisms", *Advances in Robot Kinematics*, pp.315-322.
2. A. Ghasemi, M. Eghtesad and M. Farid, 2009, "Workspace analysis for planar and spatial redundant cable robots", *Journal of Mechanisms and Robotics*, Vol.1, 044502.

3. G. Barrette and C. M. Gosselin, 2005, "Determination of the dynamic workspace of cable-driven planar parallel mechanisms", *Journal of Mechanical Design*, Vol.127, pp.242-248.
4. C. B. Pham, G. Yang and S. H. Yeo, 2005, "Dynamic analysis of cable-driven parallel mechanisms", *in the proceedings of the IEEE/ASME International Conference on Advanced Intelligent Mechatronics*, Monterey, California, USA, pp.612-617.
5. M. M. Aref, P. Gholami and H. D. Taghirad, 2008, "Dynamic and sensitivity analysis of KNTU CDRPM: a cable driven redundant parallel manipulator", *1-4233-2367-3/08 IEEE*, pp.528-533.
6. X. Diao and O. Ma, 2009, "Vibration analysis of cable-driven parallel manipulators", *Multibody System Dynamics*, Vol.21, No.4, pp.347-360.
7. Y. B. Bedoustani, H. D. Taghirad and M. M. Aref, 2008, "Dynamics analysis of a redundant parallel manipulator driven by elastic cables", *in the proceedings of* 10*th International Conference on Control, Automation, Robotics and Vision*, Hanoi, Vietnam, pp.536-542.
8. J-P. Merlet, 2008, "Kinematics of the wire-driven parallel robot MARIONET using linear actuators", *IEEE International Conference on Robotics and Automation*, Pasadena, CA, USA, pp.3857-3862.
9. S. Behzadipour, 2009, "Kinematics and dynamics of a self-stressed Cartesian cable-driven mechanism", *Jouranl of Mechanical Design*, Vol.131, 061005.
10. B. Zi, B.Y. Duan, J.L. Du and H. Bao, 2008, "Dynamic modeling and active control of a cable-suspended parallel robot", *Mechatronics*, Vol.18, pp.1-12.
11. S. Behzadipour and A. Khajepour, 2005, "A new cable-based parallel robot with three degrees of freedom", *Multibody System dynamics*, Vol.13, pp.371-383.
12. R. L. Williams II, J. S. Albus and R. V. Bostelman, 2004, "3D cable-based Cartesian metrology system", *Journal of Robotic Systems*, Vol.21(5), pp.237-257.
13. H. Liu, C. Gosselin and T. Laliberté, 2010, "A planar spring-loaded cable-loop-driven parallel mechanism", *in Proceedings of the ASME International Design Engineering Technical Conferences & Computers and Information in Engineering Conference IDETC/CIE*, Montreal, Canada, DETC2010-28424.
14. H. Liu, C. Gosselin and T. Laliberté, 2011, "A spatial spring-loaded cable-loop-driven parallel mechanism", *in Proceedings of the ASME International Design Engineering Technical Conferences & Computers and Information in Engineering Conference IDETC/CIE*, Washington, DC, USA, DETC2011-48261.